since 1961

Baltica
www.geo.lt/Baltica/baltica.htm

BALTICA Volume 19 Number 2 December 2006 : 64-71

Impact of near surface compaction on layer geometry within unconsolidated sediments, south western Baltic Sea

Nico Schmedemann, Maria–Th. Schafmeister, Gösta Hoffmann

Schmedemann, N., Schafmeister, M.-Th., Hoffmann, G. 2006. Impact of near surface compaction on layer geometry within unconsolidated sediments, south western Baltic Sea. Baltica, Vol. 19 (2), 64–71. Vilnius. ISSN 0067-3064.

Abstract Interpretation of Holocene sediments is often used for reconstruction of sea-level development in the frame of global warming subsequent to the last glaciation ca. 10000 years ago. Sea-level curves are fixed by sea-level index points. The uppermost sequence of unconsolidated sediments is characterised by highly differential compaction to about 20 m depth. Such compaction lowers the sea-level index points. This paper presents a novel method and software to calculate decompaction of any layered sequence of unconsolidated near surface sediments. Consequently depositional positions of sea-level index points are calculated. Application of the method to reconstruct the compaction behaviour of typical sediment sequences in the south-western Baltic Sea shows compaction effects of the order of several meters. Examples from a cross section and a core log respectively are presented.

Keywords *Numerical decompaction, numerical modelling, Holocene sea level, decompaction software, DeLos.*

Nico Schmedemann [nschmede@zedat.fu-berlin.de], Freie Universitaet Berlin, Institute for Geosciences, Remote Sensing of the Earth and Planets, Malteserstr. 74-100, D-12249 Berlin, Germany; Maria–Theresia Schafmeister [schaf@uni-greifswald.de], Ernst Moritz Arndt Universität Greifswald, Institute for Geography and Geology, Jahnstraße 17 a, D-17487 Greifswald, Germany; Gösta Hoffmann [G.Hoffmann@geo.uu.nl], Utrecht University, Faculty of Geosciences, P.O. Box 80115, 3508 TC Utrecht, The Netherlands. *Manuscript submitted 12 December 2006; accepted 26 December 2006.*

INTRODUCTION

Decompaction calculations are common in relation to sediment basin analysis. Especially in the frame of exploration for natural gas or oil, compaction modeling is under improvement until today (e.g. Athy 1930; Audet 1995; Goulty 1998; Hart *et al.* 1995; Springer 1993). But since these calculations are performed at depths of several hundreds to thousands meters, they do not apply to near surface sediments, where compaction effects are different. The most important difference is related to variations of layer-dependent density. Deeply buried consolidated sediments show relatively small bulk density variations of around 1.8 g/cm³ (sandstone) to 2.8 g/cm³ (chalk). In contrast, near-surface sediments show higher density variations, ranging from 1 g/cm³ (peat) to 2.5 g/cm³ (till).

Quantitative knowledge of compaction effect of near surface sediments is important for various applications. For example, when using organic deposits to reconstruct the sea-level development (e.g. Lampe 2005), not only the absolute ages of these samples (usually derived by ^{14}C-analyses) but also the exact depth at the time of deposition need to be known in order to plot sea-level index points in depth-time diagrams. Furthermore, different compactability of unconsolidated sediments in flood-basins and deltas leads to shifting of river channels and hence influences the alluvial architecture (e.g. Berendsen & Stouthamer 2000). Finally, sedimentation rates and accommodation space seems increased if older sediments are compacted.

In this paper we present a solution to calculate the effect of compaction on unconsolidated sediments and demonstrate the applicability of the approach

by presenting results from the south-west Baltic Sea coast. The work is based on a diploma-thesis (Schmedemann 2006), in which a decompaction method and software were developed. The program is named DeLos 2.0 (Dekompaktion von Lockersedimenten) and is capable of calculating decompaction from core logs, cross sections, and stacked 3D–models of layer surfaces. With this software it is possible to model and visualize changes in layer geometries caused by load-dependent effects.

STUDY AREA

The study area is located on the southwestern Baltic Sea, in the Mönchgut Peninsula of the island of Rügen (Germany) (Fig. 1). The cross section N–N' and the core log LN33 provide the data to be used

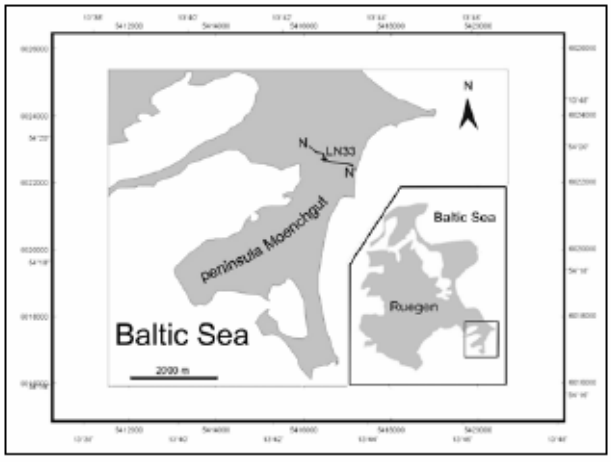

Fig. 1. Study area on the island of Rügen/ Germany at south western Baltic Sea.

in DeLos 2.0. The stratigraphic sequence comprises the Holocene and the uppermost layers of the Pleistocene. The late Pleistocene and Holocene evolution of the Mönchgut Peninsula is described in detail by Hoffmann and Barnasch (2005). Morphologically the peninsula is dominated by Pleistocene deposits (mainly till) which formed headlands. During the Holocene evolution of the Baltic Sea the headlands were partly eroded and cliffs developed. Long-shore transport led to the formation of barriers, stretching from north to south. The sediment sequence in the subsurface of the barriers compromises a lodgment till at the base, overlain by (glaci-) fluvial sands and limnic to fluvial mud or silt. A widespread peat–layer follows in the sequence and indicates the groundwater rise prior to the Litorina transgression which is interpreted at the top of the Holocene. The overlying brackish sequence comprises organic mud, silty fine sand and locally medium sand of various shallow water facies. The uppermost layer is made up of fine sand representing dunes or terrestrial peat.

METHODS

To reconstruct paleo-thicknesses from present thickness we use a simple model. It assumes an open pore space, so fluids are well described by hydrostatic assumptions. Furthermore, sediments are made up of a solid part with constant volume at all depth and a variable pore space which decreases by increasing overburden. For the decompaction calculation, first order sediment compaction parameters are needed. The compaction parameters are: initial porosity, compaction constant and sediment grain density.

Initial porosity of sediments is the ratio of pore space to bulk volume at the time of sedimentation. High initial porosities mean high potential for compaction (Allen 2000). Compaction constant is the fraction of pore space reduction (relative to total pore space) per unit increase in overburden. Thus it is an empirical coefficient describing the compressibility of the layer. A high compaction constant compared to a small one results in more loss of porosity at an equal overburden (Allen 2000).

The sediment solid density is the average density of all mineral grains the sediment type contains. Every sediment type has a characteristic combination of those three values.

The compaction parameters can be determined by analysis of density logs. Such density logs contain sediment specific dry density (ρ_{dry}) and bulk density (ρ_{bulk}) measurements (taken as closely as possible) at different overburden values. Equation (1) calculates the porosity (φ) for the density pairs. Usually 1000 kg/m³ can be assumed for water density (ρ_{water}).

$$(1)\ \varphi = \frac{\rho_{bulk} - \rho_{dry}}{\rho_{water}}$$

The resulting porosity values scatter around an exponential curve in an overburden–porosity plot. The exponential curve can be transformed to a linear form. Then a linear regression yields the compaction constant (b) as slope, while the ordinate crossing equals the initial porosity (φ_0). This allows the determination of errors as well. The equations (2) and (3) can be used for determination of the compaction parameters from the overburden (x) – porosity (y) pairs. The sample number equals unit "n".

$$(2)\quad \varphi_0 = e^{\frac{\sum x_i^2 \sum y_i - \sum x_i \sum x_i y_i}{n\sum x_i^2 - (\sum x_i)^2}}$$ (adapted from Walcher 1985)

$$(3)\ b = -\frac{n\sum x_i y_i - \sum x_i \sum y_i}{n\sum x_i^2 - (\sum x_i)^2}$$ (adapted from Walcher 1985)

The pairs of dry density (ρ_{dry}) and bulk density (ρ_{bulk}) can also be used for determination of solid density (ρ_{solid}) and its error. This is shown in equation (4).

$$(4)\quad \rho_{solid} = \frac{\rho_{bulk} - (\rho_{bulk} - \rho_{dry}) * \rho_{water}}{1 - (\rho_{bulk} - \rho_{dry})}$$

The error of the mean solid density equals the standard deviation of all computed solid densities from the dataset. The solid density of sediment is later used for calculation of bulk density at any overburden.

Best results were achieved when the overburden was expressed in units of effective stress. The effective stress is the difference between bulk stress and hydrostatic stress. The hydrostatic stress is subtracted from the bulk stress to correct the bulk stress for ascending forces due to buoyancy. Equation (5) is used to calculate the effective stress (p) as a function of depth (z). Gravitational acceleration (g=9.81 m/s²) and water density (ρ_{water}) are assumed to be constant. The bulk density (ρ_{bulk}) is calculated as equation (6) demonstrates.

$$(5)\ p = \int_0^z g\rho_{bulk}\,dz - g\rho_{water}\,z \qquad \text{(adapted from Allen 2000)}$$

Bulk density (ρ_{bulk}) is dependent of solid density (ρ_{solid}), water density (ρ_{water}) and porosity (φ).

$$(6)\ \rho_{bulk} = \rho_{solid}(1-\varphi) + \rho_{water}(\varphi)$$

Equation (7) yields the porosity (φ) from initial porosity (φ_0), compaction constant (b) and effective stress (p).

$$(7)\quad \varphi = \varphi_0 e^{(-b*p)} \qquad \text{(adapted from Hart et al. 1995)}$$

Now at any depth and thus any effective stress the sediment porosity can be calculated. For higher efficiency, the decompaction calculation proceeds from top to bottom.

The following specifications are illustrated (Fig. 2). Due to nonlinear porosity development with increasing depth it is recommended to divide the geologic layers into sublayers. To achieve desirable calculation accuracy, each layer should be thin enough that porosity differences between top and bottom of the sublayers becomes negligibly small. The sequence decompaction starts by selecting that sublayer within the present–day sediment sequence, which was earth surface at the desired ancient time slice. For this purpose, one pointer is

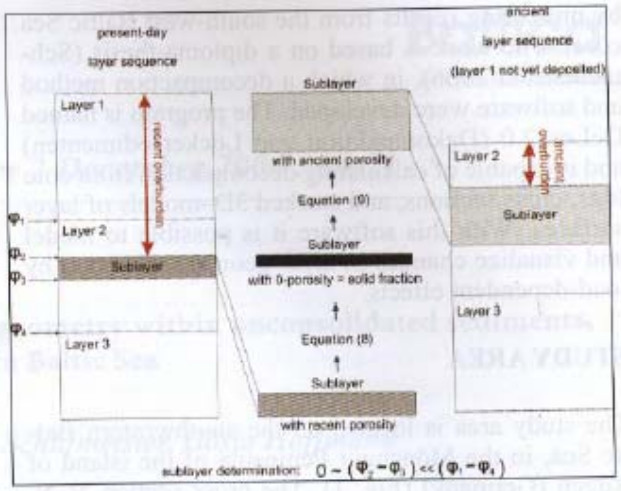

Fig. 2. Schematic diagram for the decompaction process.

set to the position of the ancient surface and a second pointer to the bottom of the same geologic layer. Then the bottom pointer is moved upwards until the porosity difference between top and bottom pointers becomes negligibly small. The porosities at the pointer positions are computed using equations (5) to (7). If the sublayer is selected, equation (8) is used to determine the thickness of its solid fraction (T_{solid}) from its recent thickness (T) and its recent porosity (φ).

$$(8)\quad T_{solid} = T*(1-\varphi)$$

The thickness of the solid fraction is the thickness of the sublayer without any pore space. Thus it is assumed to be constant at any effective stress. Because the first selected layer was the ancient earth surface, the ancient porosity equals the initial porosity. Equation (9) computes the ancient sublayer thickness (T_a) from ancient porosity (φ_a) and the thickness of the sublayer solid fraction (T_{solid}).

$$(9)\quad T_a = T_{solid} * \frac{1}{1-\varphi_a}$$

For any further sublayer the ancient porosity has to be calculated using equations (5) to (7). Such sublayers are buried by the already decompacted sublayers. When the ancient sublayer thickness is determined, it is added to the bottom of the ancient sublayer stack. Then the upper pointer in the present–day sequence is set to its lower counterpart and the lower pointer is set again to the bottom of the geologic layer to find the next sublayer. As soon as the specific geologic layer is completed, the sum of all its decompacted sublayers represents the decompacted geologic layer. The decompaction calculation continues with adapted sediment parameters until the very bottom of the whole sequence is reached.

COMPACTION BEHAVIOUR AND PROCESSES OF SEDIMENT TYPES

Brief descriptions of the sediment types involved are provided below.

Lodgement till is an unsorted sediment deposited right beneath a glacier. In the study area this type of sediment is Weichselian. It is calcareous due to reworked Upper Cretaceous sediments and occurrence of erratic blocks descending from the north and north eastern areas. This sediment is highly pre-compacted, due to the high load of the ice sheet. Hence no further compaction is expected from loads caused by a ca. 20 m thick sequence of Holocene sediments. Due to its lowermost position and rough topography, this sediment strongly influences thicknesses and occurrence of younger layers.

Clay is characterized by high grain surface areas in relation to its volume. For this reason clay typically occurs with high initial porosities as well as high compaction constants. This sediment is often located at depressions of the underlying lodgement till, which indicates a former periglacial ice lake.

Silt, sand. The compactability of silt and sand generally decreases with increasing grain-size, due to higher mass to surface ratio. These types of sediments could represent a glaciofluvial environment long before the Litorina transgression as well as developing beach ridges at different evolution stages of the Baltic Sea.

Mud. If clastic sediments are enriched in organic compounds they are referred as mud. Depending on the depositional environment mud can be separated into lacustrine or marine mud. The compactability of mud depends on the organic carbon content: increasing organic carbon content increases the compactability. In addition gaseous enrichments which occur due to chemical decay of organic content influences the compactability of organic sediments. This results in a high variability of initial porosity and compaction constant of mud. Mud indicates a water depth of some meters and thus the transgression phase at the study area.

Peat is made up of partially decayed plant remains. Peat compaction is highly variable in dependence of tissue resistance of the plant remains. Peat grows in water saturated environments almost levelled to ground water surface. Therefore peat is an important indicator for ancient water levels. The density is almost the same as water. Consequently peat shows no autocompaction as long as it is not subjected to any overburdens. Peat compacts to a much higher extent than any other sediment type. Even a lowering of groundwater level leads to peat compaction, because the uppermost peat sections are no longer subjected to buoyancy forces.

As already mentioned, chemical decay is a major impact to peat development. It was stated that significant amounts of carbon compounds are released from plant remains by chemical decay (Succow & Joosten 2001). The decay rate depends on the appearance of reactant materials as well as on temperature (Nadon 1998). Therefore calculated initial peat thicknesses from present–day peat thickness are only minimum assessments, because it is unknown how much material was lost due to chemical decay.

Peat indicates a rising groundwater level and thus the beginning of the Litorina transgression at the study area.

Used compaction parameters. The sediment dependent compaction parameters were used for decompaction calculation (Table 1). Only for two sediment types (lacustrine and marine mud) were sufficient density data available. For those types compaction parameters were obtained by analysis of density logs as described and thus determination errors can be quantified. The other values were estimated by experience or taken from literature (Schmedemann *et al.* 2005). Therefore no errors for those values are available. For best results it is recommended that for every drilling to be decompacted only sediment parameters measured on location to be used. Otherwise results could be corrupted by spatially varying sediment properties.

Table 1. Sediment compaction parameters used in decompaction modelling.

Sediment type	Initial porosity [%]	Compaction constant [1/Pa]	Solid density [g/cm³]
Lodgement till	10	1.00E-05	2.65
Clay	82	8.00E-03	2.10
Silt	56	1.30E-04	2.65
Fine sand	34	7.72E-03	2.14
Sand	34	7.72E-03	2.14
Coarse sand	34	7.72E-03	2.65
Grevel	50	1.00E-04	2.65
Marine mud	72 (+/-0.39)	1E-03 (+/- 3 E-04)	2.5 (+/- 0.16)
Lacustrine mud	89 (+/- 0.4)	6E-03 (+/- 3 E-04)	2.4 (+/- 0.11)
Peat	90	1.70E-02	1.00

RESULTS

Compaction behavior of sediments in core log LN33

The core log LN33 (Hoffmann 2004) is part of cross section N–N' (Hoffmann 2004) described below. The depth of layer surfaces is shown at 6 time steps (Table 2). At each time step the deposition of the respective top layer was just completed. The last time step equals the present–day layer sequence. The mentioned depths are related to the present–day m.s.l. at that region. The time steps are defined by facies change. Hence the time step borders comprise not the same time intervals, due to changing sedimentation rates.

Table 2. Depth of layer surfaces [m.s.l.] of core log LN33 (data base: Hoffmann 2004).

Time step	1	2	3	4	5	6
Layer						
Peat						0.40
Sand					0.20	0.20
Mud				-2.43	-3.85	-3.85
Peat			-2.38	-3.66	-5.00	-5.00
		-4.70	-4.70	-5.02	-5.45	-5.45
Silt	-5.68	-5.68	-5.68	-5.68	-5.70	-5.70

A reconstruction of the compaction development at drill site LN33 is shown (Fig. 3). Time steps are divided to produce a higher resolution for analyzing compaction effects within the layer sequence. Starting at the left border, we look back to that time as the first centimeter of the whole sediment sequence was deposited. Every step to the right adds 1 cm of sediment atop the sequence. At the same time the layer thicknesses are corrected for compaction effects. To the very right the present–day sediment sequence is drawn. Due to the high resolution actually no steps are visible. In this way stepwise lowering of layer borders affiliates to continuous lines, which demonstrates the compaction, had driven lowering of layer surfaces. The line which borders the sediment sequence to the top is always the earth's surface. Because every step adds 1 cm of sediment, the time axis shows an uneven time scale. This is due to a variable sedimentation rate.

In general, the rate of compaction decreases by decreasing sediment porosity. This is indicated by flattening of the layer surfaces with time and thus increasing overburden.

Detailed analyses of the silt layer shows that its compaction is negligibly small. It experienced an almost compaction-free accumulation. That is visible by the straight line, which resample earths surface at the time as this layer was build. The surface of the silt layer was lowered only by 2 cm since the time it was covered by lacustrine mud.

The compaction development of the lacustrine mud layer is mainly characterized by the covering layers. As long as peat grows atop the lacustrine mud no surface lowering of the lacustrine mud layer happens. This is because peat produces no effective stress in a water saturated environment. As mud deposition started, the mud stresses the subjacent layers. This could be recognized in lowering of the surface of lacustrine mud. As sand replaced mud sedimentation, the higher density of sand compared to that of mud led to an increasing rate of surface lowering of the lacustrine mud layer. Its total lowering is 77 cm. This means 75 cm of total lowering are caused by compaction of the lacustrine mud layer and 2 cm are caused by compaction of the underlying silt, as already mentioned. The lacustrine mud is covered by 232 cm of peat at its initial thickness. Due to compaction the peat surface is lowered by 262 cm in total. 187 cm of total surface lowering is caused only by compaction of peat itself. The rest is mainly caused by compaction of the underlying lacustrine mud. Further, the lowering

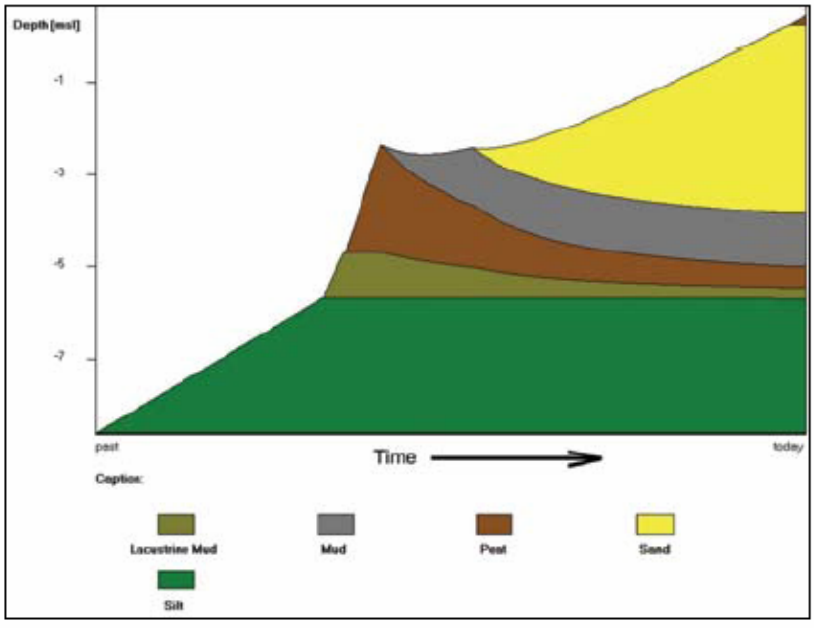

Fig. 3. Model of compaction development at drill site LN33.

rate does not flatten constantly but shows an increasing value as sand replaces mud sedimentation. This is due to a higher sand density compared to that of mud.

The total surface lowering of the mud layer is 142 cm. The thickness decrease of the mud itself, however, contributes only 8 cm to that amount, i.e. app. 6 percent. Thus 134 cm or 94 percent of mud surface lowering is caused by compaction of subjacent layers, especially the peat layer. Due to initially strong compaction of subjacent peat, the bottom of the mud is lowered slightly faster than sedimentation; the newly developed sedimentation space is not fully occupied. In that way the surface of the mud layer was lowered while mud sedimentation was still going on. The result of this action is a lowering of mud deposition level, beginning at –2.38 m m.s.l. to –2.43 m m.s.l. at the end of mud sedimentation. While this time period an initial mud layer thickness of 123 cm was build up. It should be mentioned, that mud already compacts while it is deposited. This effect is accounted as well by DeLos 2.0. The sand layer, which buries the mud layer, supplies the most stress to the subjacent layers. This is caused by its high density as well its remarkable thickness of 405 cm. The present–day top layer is made up of peat, which causes no compaction to subjacent layers at all. This is due to its neutral behavior with respect to effective stress.

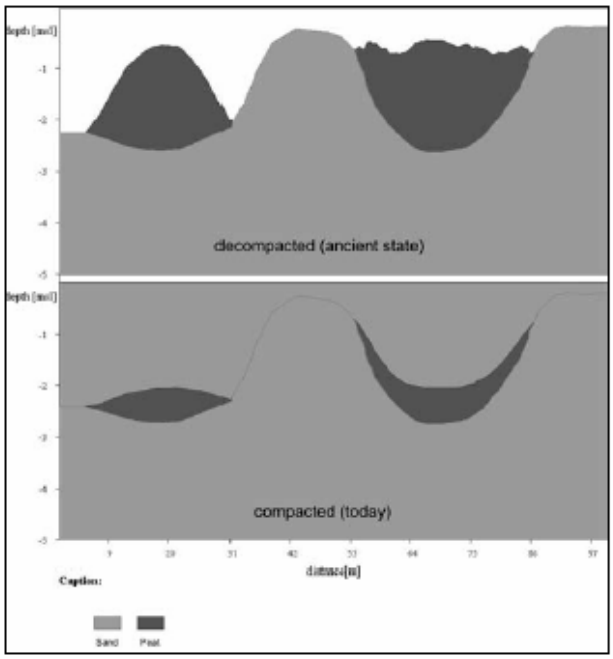

Fig. 4. Comparison between two fictitious peat lenses embedded in sand. Both lenses are known with the same center thickness, the spikes are interpolated.

Compaction behavior and geometry change of sediments in cross sections

By decompaction of many adjacent core logs a decompaction of a cross section can be performed. This allows for a plausibility check as whether a cross section may have existed as calculated (by DeLos 2.0) or not, just by geometric appearance. This is demonstrated for a fictitious example where both peat lenses are embedded in sand and only their center thickness is known (Fig. 4). So their spikes are free for interpolation. If the lens geometry is interpolated in the left way as often seen in geologic cross sections, the decompacted peat lens has a hill like appearance which is hard to explain. If instead a parabolic lens shape is assumed, as on the right side of the figure, the decompacted peat lens shows an almost horizontal surface which is more consistent with common peat forming processes.

Cross section N–N' (Hoffmann 2004; section 0 m–1260 m)

The cross section N–N' is pictured at its decompacted and present–day state (Fig. 5). The time slice for the decompacted state equals the time as peat sedimentation was just finished. At the center of the cross section the till layer shows a depression. At this depression a lacustrine mud, peat, marine mud and sand were deposited. Here the focus is on the peat layer which was deposited direct onto till at the margins of the depression. As mentioned above, till is incompactable at given circumstances. This means that the points of the peat-till contact were not moved due to compaction. Based on standard peat forming processes it is assumed, that peat surfaces in this region are highly correlated to groundwater development. According to this, the peat surface should be as horizontal as the groundwater surface was. So the peat–spikes should be almost at the same height level and be connected by a more or less horizontal surface at the decompacted state (Fig. 5).

The stress related decompaction calculation performed by DeLos 2.0 is indeed able to reconstruct the paleo–surface of the peat layer as it was assumed. The short wave roughness of the modeled peat surface is due to small errors in drawing the present–day cross section. The long wave roughness is caused by different possibilities. On the one hand its possible that the interpolations between the core logs are incorrect, on the other hand sediment properties could show spatial variability, which influences their compactability. These errors are amplified by the amount of calculated compaction effect. Such errors are large in highly compacted layers.

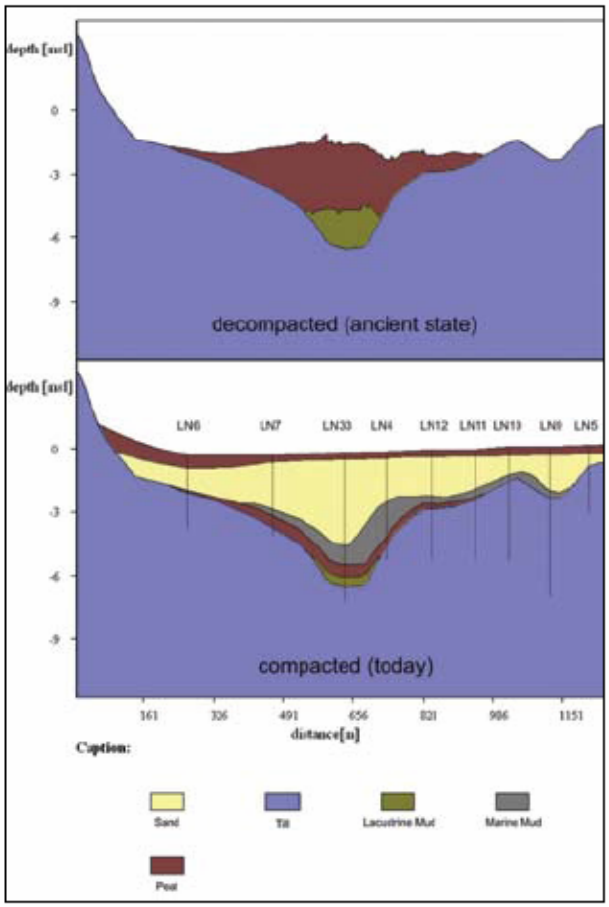

Fig. 5. Cross section N-N' at state of decompacted peat layer and today.

INTERPRETATION

In the field of reconstruction of the sea level development from sea–level–index points, the consideration of compaction effects could lead to significantly different RSL curves. This is due to the fact that the often used ^{14}C–analyses are dependent on organic enriched sediments, which in turn are well compactable as shown. Even OSL–dated sediments, which are usually less compactable, could be affected by compaction. This happens if well compactable material occurs within the subjacent sediment sequence. RSL curves which are corrected for compaction would show a faster sea level rise than uncorrected curves. In the study area the decompacted elevation level of the peat deposited prior the transgression is increased for the given ages. Thus the sea level had to be higher than previously thought at those times. Another aspect in this field is the possibility that isolated water bodies, postulated by different water levels could show the same water level after consideration of compaction. In our study there were examples in which compaction lowered the altitude of a sea-level-index point by almost 7 m. Without decompaction this sample was an outlier. After decompaction it fits perfectly into the dataset.

Consideration of compaction with respect to the development of river systems could help to explain the development of flood plains and river deltas. Due to permanent shifting of river channels in the course of deltaic evolution and very effective sediment differentiation, such areas are characterized by highly variable layer geometries. Because of less compactable sand deposited within the river channels and high compactable flood plain deposits, these setting results in highly variable compactability. Permanent sedimentation of clastic and therefore dense sediments leads to compaction of this variable compactable ground and affects in this way the river profile in different ways.

Relatively dense sediments compacts their highly compactable underground very intensive. The top of those layers are lowered as well, if the bottom boundary lowering rate of the denser sediment layer exceeds the sedimentation rate at its top. In that case more accumulation space is provided by compaction. Thus, unusually thick units of distinct layers might be deposited.

CONCLUSIONS

The given examples show that compaction amounts of till are negligible small. Silt and sand compacts by only a few centimeters, while the thickness of mud layers shrinks tens of centimeters. However the lower peat compacts on the order of hundreds of centimeters, while the upper peat at earth surface didn't compact at all. Stress related decompaction calculation as done by DeLos 2.0 is capable to model reliably the ancient layer geometry. This were demonstrated by geometric ratios in cross section N–N' with respect to the knowledge of peat forming processes. The cross section decompaction can handle complex relationships between intercalated layers of different sediment types. Further the high resolution core log decompaction is capable to reconstruct the compaction history in detail. At core log LN33 it turns out that sedimentation of dense material like sand onto a high compactable layer sequence could increase compaction rates again. This example shows that surface lowering of a given layer is dependent not only on its own compactability. It also has to be handled with respect to subjacent layers as well as the overburden.

The differential compaction of any given layer sequence of unconsolidated sediments can be handled by DeLos 2.0. That is possible, because the compaction behavior of sediments in dependence of the overburden is defined by only two values: initial pore space and compaction constant. Both values can be calculated by analysis of density core logs. This analysis can be performed by DeLos 2.0 but this software allows presetting values as well. DeLos 2.0 is further capable of performing decompaction not only of 1D and vertical 2D but also of 3D data sets.

Acknowledgements

Special thanks for revising this paper are directed to D. Tetzlaff, J.Harff and reviewers. For providing web space we thank the Baltic Sea Research Institute, Warnemuende.

Authors diploma thesis as well the software DeLos 2.0 are free for download (http://www.io-warnemuende.de/projects/sincos/archive/schmedemann2006.pdf ; http://www.io-warnemuende.de/projects/sincos/archive/delos2.zip).

References

Allen, J.R.L. 2000: Holocene coastal lowlands in NW Europe: autocompaction and the uncertain ground. *In* Pye,K. & Allen, J.R.L. (eds.), *Coastal and estuarine environments: sedimentology, geomorphology and geoarchaeology.* Geological Society Special Publication 175, London, 239–252.

Athy, L.F. 1930: Density, porosity, and compaction of sedimentary rocks. *AAPG Bulletin 14(1),* 1–24.

Audet, D.M. 1995: Mathematical modelling of gravitational compaction and clay dehydration. *Geophysical Journal International 122(1)*, 283–298.

Berendsen, H. J. A., Stouthamer, E. 2000: Late Weichselian and Holocene palaeogeography of the Rhine-Meuse delta, The Netherlands. *Palaeogeography, Palaeoclimatology, Palaeoecology 161,* 311–335.

Goulty, N.R. 1998: Relationships between porosity and effective stress in shales. *first*

break 16(12), 413–419.

Hart, B.S., Flemings, P.B., Deshpande, A. 1995: Porosity and pressure: Role of compaction disequilibrium in the development of geopressures in a Gulf Coast Pleistocene basin. *Geology 23 (1),* 45–48.

Hoffmann, G., 2004: *Rekonstruktion und Modellierung der Küstenevolution im Bereich der Pommerschen Bucht in Abhängigkeit von holozänen Meeresspiegelschwankungen.* PhD thesis Ernst-Moritz-Arndt-Universität Greifswald. 135 pp.

Hoffmann, G., Barnasch, J. 2005: Late Glacial to Holocene coastal changes of SE Rügen Island (Baltic Sea, NE Germany). *Aquatic Sciences 67,* 132–141.

Lampe, R. 2005: Lateglacial and Holocene water–level variations along the NE German Baltic Sea coast: review and new results. *Quaternary International 133–134,* 121–136.

Nadon, G. C. 1998: Magnitude and timing of peat–to–coal compaction. *Geology 26 (8),* 727–730.

Schmedemann, N., Dietrich, H., Hoffmann, G. & Schafmeister, M.–Th. 2005: Computerized de-compaction of Holocene sediments. *In* Cheng, Q. & Bonham-Carter, G. (eds.), *Proceedings of IAMG'05: GIS and Spatial Analysis, 1,* Toronto, Wuhan, 422–427.

Schmedemann, N. 2006: Numerisches Modell zum Kompaktionsverlauf in oberflächennahen Lockersedimenten. Diploma thesis Ernst-Moritz-Arndt-Universität Greifswald. 95 pp.

Springer, J. 1993: Decompaction and backstripping with regard to erosion, salt movement, and interlayered bedding. *Computers & Geosciences 19(8)*, 1115–1125.

Succow, M. & Joosten, H. 2001: *Landschaftsökologische Moorkunde.* E. Schweizerbart'sche Verlagsbuchhandlung, Science Publishers, Succow, M. & Joosten, H. (eds), Stuttgart. 622 pp.

Walcher, W. 1994: *Praktikum der Physik.* B.G. Teubner, Stuttgart. 415 pp.